Biophysical Chemistry 152 (2010) 89–98

Contents lists available at ScienceDirect

Biophysical Chemistry

journal homepage: http://www.elsevier.com/locate/biophyschem

Effects of amino acid transport limitations on cultured hepatocytes

Hong Yang [a], Marianthi G. Ierapetritou [a], Charles M. Roth [a,b,*]

[a] Department of Chemical and Biochemical Engineering, Rutgers, the State University of New Jersey, NJ, USA
[b] Department of Biomedical Engineering, Rutgers, the State University of New Jersey, NJ, USA

ARTICLE INFO

Article history:
Received 24 June 2010
Received in revised form 9 August 2010
Accepted 10 August 2010
Available online 17 August 2010

Keywords:
Cultured hepatocytes
Amino acid transport
Metabolic flux

ABSTRACT

Amino acid supplementation has been shown to enhance the liver-specific functions of cultured hepatocytes during plasma exposure. However, their transport through the cell membrane may restrict their availability for hepatic metabolism. Here, we focus on transport constraints related to uptake of the neutral amino acids and their impact on hepatic metabolism and liver-specific functions. Under varying combinations of their medium concentrations, we found that transport competition exists among the three amino acids alanine, serine and glutamine and that the resulting capacity constraints affect the urea and albumin production of cultured hepatocytes. Regression equations were developed to quantify these constraints and were incorporated with other constraints (mass balance, measured flux data and reaction directionality) within a multi-objective flux balance framework to understand how amino acid transport constraints propagate through central hepatic metabolism and to predict refined amino acid supplementations for specific hepatocyte design objectives.

1. Introduction

The performance of cultured mammalian cells is tightly connected to the amino acid supplementation employed in the culture medium. For industrial cell culture processes, this supplementation can be adjusted using a factorial design methodology. However, such an approach does not provide understanding into the effects of various supplementations and thus must be restarted if the operating conditions or desired outputs change. In the case of primary hepatocytes being cultured for use in a bioartificial liver (BAL) device environment, an empirically derived amino acid supplementation has been shown to counteract the detrimental effects of plasma exposure [1]. Furthermore, we have recently shown that an amino acid supplementation designed using a rational optimization approach can lead to improvements in targeted metabolic objectives [2].

Metabolism of amino acids is tied intimately to their transport into or out of the cell, utilizing specific transporters that bind the amino acids and mediate their passage across the cell membrane. Transporters with the same recognition properties form a transport system. Amino acid transport is generally based on their ionic charge—neutral, cationic and anionic—and is mediated by independent transport systems with overlapping specificities as summarized in Table 1 [3–5]. Since several amino acids share a particular transporter, its capacity affects the transport of each amino acid that utilizes it. Thus, an excess of one amino acid may inhibit the uptake of the other amino acids that are mediated by the same transport system [6]. For hepatocytes, there is evidence to suggest that amino acids sharing System A may be susceptible to competitive capacity constraints. For example, it has been shown that the transport rate is a controlling step for alanine metabolism [7], and a similar conclusion was drawn for glutamine [8]. Alanine and glutamine transport is mediated by the same transport system A with serine [9].

In order to assess the influence of shared system A transport on hepatocyte metabolism, the effect of varying combinations of alanine, serine and glutamine on hepatocyte metabolism was measured. Indeed, competitive relationships were observed, and these were captured mathematically using least-square regression equations, which successfully explain the variance and dependence in amino acids transport fluxes (alanine, serine and glutamine). Furthermore, these amino acid transport constraints are incorporated together with other constraints including mass balances, measured data and reaction directionality within a multi-objective metabolic flux balance model to investigate the effect of transport constraints and to predict the amino acid supplementation of alanine, serine and glutamine for maximum urea production and fatty acid oxidation.

2. Materials and methods

2.1. Design of experiments: amino acids transport

Hepatocytes were isolated from adult male Fisher F344 rat (150–200 g) based on the two-step collagenase-perfusion method via the portal vein described previously [10]. Cells were cultured in a collagen sandwich configuration at a density of 1×10^6 cells/mL in six-well plates. Initially, hepatocytes were cultured in the standard hepatocyte C + H medium, which consists of DMEM supplemented with 10% heat inactivated fetal bovine serum (FBS), 7.0 ng/mL glucagon, 7.5 g/mL

* Corresponding author. 599 Taylor Road, Piscataway, NJ 08854, USA. Tel.: +1 732 445 4500x6205.
E-mail address: cmroth@rutgers.edu (C.M. Roth).

0301-4622/$ – see front matter © 2010 Elsevier B.V. All rights reserved.
doi:10.1016/j.bpc.2010.08.004

Table 1
Amino acid transport systems [3–5].

Transport system	Name	Amino acid	Ion sensitive	Others
Neutral	A	ALA, SER, GLN	Na^+	pH-sensitive
	ACS	ALA, SER, CYS	Na^+	pH not affect
	N	GLN, ASN,HIS	Na^+	A/N transport [25,26]
	L	Branched-chain and other aromatic amino acids	–	Poorly metabolized and not accumulated in hepatocytes
Gly	Gly	Glycine	Na^+, Cl^-	
Cationic	y+	ARG, LYS, ORN	Na^+, Cl^-	CAT2 in hepatocytes
Anionic	X^-_{AG}	GLU, ASP	Na^+, K^+	EAAT 1 to 5

hydrocortisone, 20 g/L epidermal growth factor, 200 U/mL penicillin, 200 g/mL streptomycin, and 500 mU/L insulin. Hepatocytes were exposed to this medium for three days with daily medium change. We determined in pilot experiments that this provided sufficient time for fluxes of glucose, urea, glycerol, free fatty acids and the protein albumin to stabilize and remain constant (data not shown).

RPMI_1600, plus 10% FBS and the same concentrations of glucagon, EGF, insulin, and glucose as C + H medium, was used to wash hepatocytes three times at 1 hour intervals. Next, cells were cultured in media with varying combinations of alanine, serine and glutamine supplementation (total 33 combinations, in Appendix A), for an additional three days with daily medium change. At the end of the experiment, the supernatant was collected and stored at 4 °C for later assay.

2.2. Design of experiments: amino acids supplementation

Hepatocytes were cultured using the collagen sandwich method [10] at a density of 1×10^6 cells/mL in six-well plates. After the second gel layer solidified, 0.8 mL fresh C + H medium (described in Section 2.1) with 0.05 mU/mL insulin (low insulin, LI) or 500 mU/mL (high insulin, HI) was added. The medium was exchanged every day. After 6 days of preconditioning, hepatocyte cultures were exposed to plasma with hormone supplementation including 7.5 g/mL of hydrocortisone and 0.05 mU/mL of insulin (WH) or without hormone supplementation (NH). Treatment groups varied in the amino acid supplementation in the plasma, comparing "designed" amino acid supplementation (DAA) based on a rational design approach described in our previous work [2], and "reference" amino acid supplementation (RAA) based on published data [1]. The medium concentrations corresponding to each amino acid supplementation are given in Appendix B. Medium exchanges were performed daily over the five days of plasma exposure. At the end of the experiment, culture supernatants were collected and stored at 4 °C prior to analysis.

2.3. Biochemical assays

In the conditioned culture medium, urea was measured using a commercial kit (Sigma, St. Louis, MO) which is based on the reaction of diacetyl monoxime with urea. Albumin production was quantified by an enzyme-linked immunosorbent assay (ELISA) using purified rat albumin (MP Biomedicals, Solon, OH) and peroxidase-conjugated antibody for detection (MP Biomedicals, Solon, OH).

Amino acids were labeled with AccQ reagent (Waters Corporation, Milford, MA) and separated using a Beckman Coulter HPLC system with a fluorescence detector (Waters 470, Waters Corporation, Milford, MA) scanning at 250/395 nm excitation/emission. Serial dilutions of standards were used to construct a calibration curve for each analyte, with the linear portion utilized for measurements. The concentrations of amino acid/ammonia in the fresh or spent medium were determined using these standard curves, with sample dilutions performed as necessary to operate within the linear range.

In addition, for the experiment of the amino acid supplementation during plasma exposure, the concentrations of glucose, lactate, glycerol, and glutamine were measured colorimetrically using commercial kits (Sigma, St. Louis, MO). Enzymatic kits were utilized for the measurement of cholesterol (BioAssay System, Hayward, CA), acetoacetate, β-hydroxybutyrate, triglycerides (Stanbio, Boerne, TX), and free fatty acids (Roche, Indianapolis, IN).

2.4. Transport constraints

A quadratic model is used to quantify the transport limitations that exist between amino acid uptake/secretion and their concentrations in the cultured medium, as follows:

$$v_l = \beta_0 + \sum_k \beta_k C_k + \sum_i \sum_j \beta_{ij} C_i C_j + e; \quad (i,j,k,l) = \{\mathrm{Ala}, \mathrm{Ser}, \mathrm{Gln}\}. \quad (1)$$

The regression parameters were estimated from a set of known values of concentrations of alanine (C_{Ala}), serine (C_{Ser}), and glutamine (C_{Gln}) supplied in the medium and their corresponding measured uptake/secretion fluxes (v_l) using the method of least squares regression, as implemented in SAS/STAT (SAS Institute, Inc., Cary, NC). A Student's *t*-test was used to identify which terms contribute significantly to the flux values. Terms with $p<0.05$ were considered to be significant, while the others were excluded from the model.

2.5. Metabolic flux modeling

In this work, we measure and interpret the metabolism of hepatocytes in terms of their fluxes as opposed to metabolite concentrations as would be done in a metabolomics approach. The advantages of utilizing metabolic flux are that the flux, or throughput, is more representative of the metabolic phenotype and that measurement of some flux values can be used to infer the values of additional fluxes through material balances, enabling a more complete view of cellular metabolism. Metabolic flux modeling involves construction of a metabolic reaction network that captures the reactions of interest and the formation of mass balances around each of the internal metabolites, expressed as

$$\frac{d\mathbf{X}}{dt} = \mathbf{S}\cdot\mathbf{v}, \quad (2)$$

where **X** is the vector of metabolite concentrations, **S** the stoichiometric matrix and **v** the vector of fluxes [11]. This equation is applied in the pseudo-steady-state, removing the metabolite concentrations from explicit consideration. The flux vector **v** is partitioned into measured and unknown fluxes and the resulting system of linear equations can be solved algebraically if the number of unknown fluxes is equal to the number of balance equations. Otherwise, optimization approaches are used to solve the equations for an assumed objective function and/or subject to additional physicochemical constraints.

The basic hepatic network used in this work builds upon previously reported hepatic networks [1,12–15] and involves 46 intracellular metabolites, and 78 reactions (30 reactions with measurement data, 48 reactions with unknown fluxes as listed in Appendix C). The pathway for gluconeogenesis, and not glycolysis, is used in this work, based on previous studies of hepatocyte cultures exposed to plasma using amino acid supplementation (Yang et al., submitted for publication). The other reactions included those involved in tricarboxylic acid cycle (TCA), urea cycle, amino acid uptake/secretion and catabolism, oxygen uptake, electron transport system, pentose phosphate reactions (as a lumped group), ketone body synthesis, fatty acid, triglyceride (TG) and glycerol metabolism.

The constraints derived to express the transport limitations of amino acids are incorporated into a flux balance optimization framework to investigate the effects of amino acid supplementation

on the objectives of urea production and fatty acid oxidation. The optimization model is as follows:

$$\begin{aligned} &\max\{v_{urea}, v_{Fatty\ \ Acid\ \ Oxidation}\} \\ &s.t. \quad \sum_{j=1}^{N} S_{ij}v_j = 0, \quad i\in M \\ &\quad v_j^{\min} < v_j < v_j^{\max}, \quad j\in K \\ &\quad v_k = f(C_{Ala}, C_{Ser}, C_{Gln}) \quad k\in K' \end{aligned} \tag{I}$$

where S_{ij} is the stoichiometric coefficient of metabolite i in reaction j; $v_j^{\min}$ and $v_j^{\max}$ are lower and upper bounds of reaction j, respectively; M is the set of metabolites; N is the total number of reactions involved in the hepatic network; K is the set of constrained reactions (based on measurements from amino acid supplementation experiment and/or irreversibility); and K' is the set of additional transport constraints generating by nonlinear least-square regression (Eq. (1)). The main assumptions for the development of model (I) are as follows:

(1) Metabolism is assumed to be at a pseudo-steady-state. The pseudo-steady-state approximation is considered to be valid because the concentrations of intracellular metabolites are very small (~nmol/million cell) compared to their turnover, relative flux (~μmol/million cell/day)×measurement time (1 day) [2,16]. The time allowed for culture stabilization (three days before amino acid transport experiments and six days of preconditioning before plasma exposure) and the stable collagen sandwich culture configuration combine to support this assumption. Furthermore, it should be noted that primary hepatocytes are non-dividing cells so that the dilution effect due to changing cell number was not considered.

(2) Urea maximization is a reasonable objective since it is often used as a marker of hepatocyte function that reflects their ability to perform ammonia detoxification and is typically correlated with a healthy phenotype of hepatocytes [2]. Fatty acid oxidation was identified as an additional metabolic objective to represent the reduction of lipid accumulation with amino acid supplementation observed in our previous work [2]. Therefore, both of them are considered as objective functions in this study. While other metabolic objectives such as xenobiotic metabolism are relevant to hepatocyte function [17], we utilize urea production in order to allow integration of transport constraints quantified here with our previous work focusing on urea [2].

(3) Based on our previous results using amino acid supplementation, in this work we derived the bounds in model (I) using the ensemble of measurements from conditions with amino acid supplementation (DAA and RAA) and varying in their insulin preconditioning (HI and LI) and hormone supplementation during plasma exposure (NH and WH). The range of these experimental measurements defines the flux bounds representing the observed metabolic capabilities.

(4) The reversibility of each reaction is determined based on the information given in the metabolic map of KEGG [18]. Reversible reactions are allowed to take either positive or negative values, whereas flux values for irreversible reactions are restricted in accordance with their KEGG reaction directionality.

(5) Albumin synthesis, which is an important liver-specific function [2,13,15] but makes a modest contribution to central metabolism due to its comparatively lower molar flux, is considered constant in model (I) and equal to the value at the designed amino acid supplementation. Likewise, we assume that the reactions considered in the network account for most of the metabolic activity, on a molar basis, for the metabolites balanced in the model. This assumption is based on the prior experience of ourselves and others in working with essentially the same network to describe hepatocytes both in vitro and in vivo [1,2,12,17].

Model (I) corresponds to a nonlinear programming (NLP) problem, since the transport constraints are nonlinear function. It was solved by the ε-constraint method [19], which maximizes a primary objective while it converts another objective into a constraint as follows:

$$\begin{aligned} &Max \quad v_{urea} \\ &s.t. \quad \sum_{j=1}^{N} S_{ij}v_j = 0, \qquad i\in M \\ &\quad v_j^{\min} < v_j < v_j^{\max} \qquad j\in K \\ &\quad v_k = f(C_{Ala}, C_{Ser}, C_{Gln}) \quad k\in K' \\ &\quad v_{Fatty\ \ Acid\ \ Oxidation} \geq \varepsilon. \end{aligned} \tag{II}$$

Choosing a different value of parameter ε results in the determination of a set of Pareto-optimal solutions where urea production and the flux of fatty acid oxidation are best compromised.

3. Results

3.1. Amino acid transport constraints

Hepatocytes were cultured in the collagen sandwich configuration, which is known to provide stable differentiated function over several weeks [10], and conditioned in C+H medium for three days to stabilize the culture. After this time, hepatocytes were exposed to a combinatorial set of alanine, serine and glutamine levels in RPMI_1600 medium for an additional three days with daily exchange of medium. At the end of the experiment, alanine, serine and glutamine fluxes were calculated from their measured concentrations in the collected supernatants (Appendix A). Because the values are calculated from differences in metabolite concentrations between days 2 and 3 of exposure, transients should be dissipated but the values should nevertheless be considered as averages over the course of one day [20]. Glutamine levels were about an order of magnitude greater than serine and alanine levels in accordance with the levels used in previous supplementations [2,21].

Flux measurements demonstrated that hepatocytes import alanine from the supplied medium when the concentration of glutamine is low. However, alanine is no longer imported but rather secreted into the medium when the concentration of glutamine increases (Fig. 1A). Similar behavior is observed for the serine flux (Fig. 1B), which suggests that both alanine and serine uptake are inhibited by high glutamine levels. It is further shown that hepatocytes have limited uptake capacity for glutamine and that the rate of glutamine uptake is roughly constant when glutamine supplementation in the medium is increased up to 4 mM (Fig. 2A and B). This effect is independent of alanine and serine supplementation in the medium. Although present at a lower level than glutamine, serine also inhibited the intake of alanine (Fig. 3A). Serine flux was unique in that it exhibited a maximum with respect to serine concentration (Fig. 3B), indicating the existence of a possible feedback regulation.

The effect of transport competition on the liver-specific functions, urea and albumin, was determined. Using a range of alanine and glutamine supplementation levels, it was found that urea production initially increases with glutamine supplementation, attaining a maximum value when the glutamine concentration is close to 4 mM (Fig. 4A). Higher levels of glutamine supplementation lead to a decline in the urea production. However, urea production is not affected significantly by varying levels of serine and glutamine supplementation (Fig. 4B). It appears in this case that lowered serine uptake can be compensated by the production of serine from glycine (v_{u19}). Albumin synthesis decreases with increasing glutamine supplementation and is independent of alanine and serine concentration within the range of values tested (Fig. 5A, B).

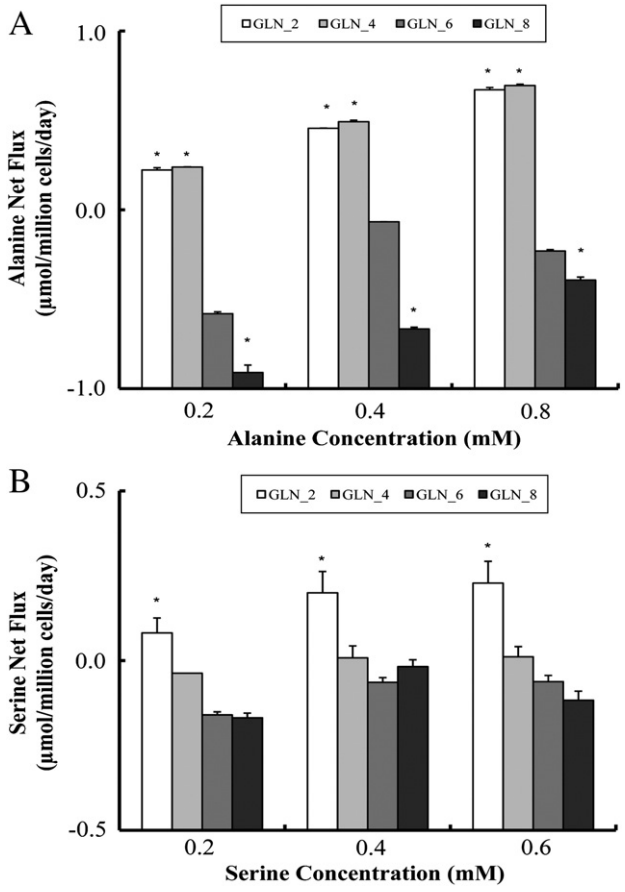

Fig. 1. Alanine and serine fluxes are affected by glutamine level: (A) Alanine net fluxes under varying combinations of alanine and glutamine concentrations in the medium; (B) serine net fluxes under varying combinations of serine and glutamine in the medium. Legend indicates glutamine concentration in units of mM, and asterisks (*) indicate significant differences ($p<0.05$) in fluxes between the indicated glutamine level and a supplied glutamine level of 6 mM for the same alanine and serine supplementation.

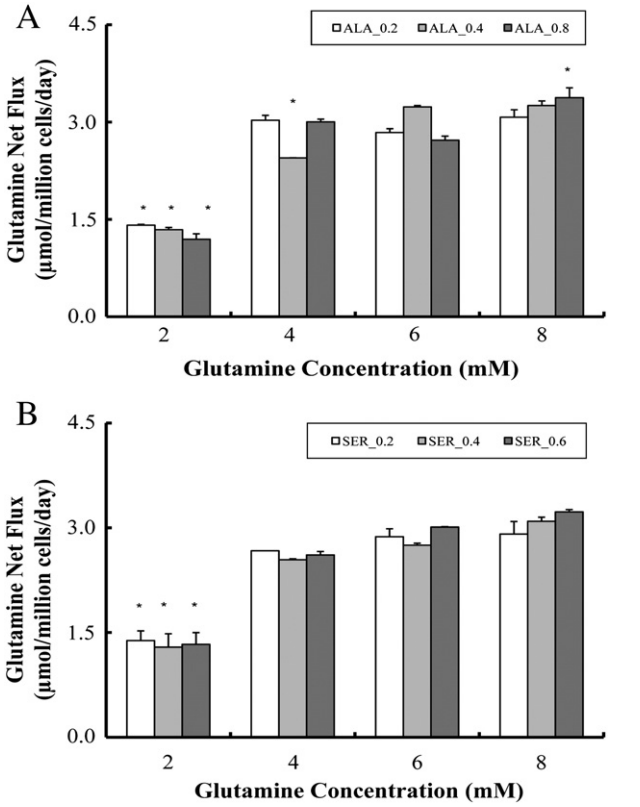

Fig. 2. Glutamine uptake is capacity limited: (A) Glutamine flux under varying combinations of alanine and glutamine concentrations in the medium; (B) glutamine flux under varying combinations of serine and glutamine concentrations in the medium. Legend indicates glutamine concentration in units of mM, and asterisks (*) indicate significant differences ($p<0.05$) in fluxes between the indicated glutamine level and a supplied glutamine level of 6 mM for the same alanine and serine supplementation.

In order to investigate the effects of these restrictions on the hepatic network during plasma exposure, a nonlinear regression model was used to fit these three amino acid fluxes as a function of their supplied concentrations in the medium; those equations were incorporated into the flux analysis model as constraints. All the experimental data in Appendix A were used to calculate the parameters in the regression model in Eq. (1), and only those significant parameters (with p value less than 0.05) are shown for nonlinear transport constraints as follows:

$$v_{Ala-uptake} = -0.218 + 2.910C_{Ala} - 1.859C_{Ala}^2 - 0.019C_{Gln}^2 - 1.538C_{Ala}C_{Ser} + 0.062C_{Ser}C_{Gln} \quad (3)$$

$$v_{Ser-uptake} = -0.323 + 2.189C_{Ala} - 2.185C_{Ala}^2 + 4.000C_{Ser} - 4.832C_{Ser}^2 - 0.210C_{Gln} + 0.017C_{Gln}^2 \quad (4)$$

$$v_{Gln-uptake} = -0.620 + 1.118C_{Gln} - 0.081C_{Gln}^2 + 0.005C_{Ala}C_{Gln} - 0.042C_{Ser}C_{Gln}. \quad (5)$$

The high values of coefficient of determination (R^2) for these nonlinear regression models ($R^2 \geq 0.88$) imply that most of the variability in amino acid transport rate (v) can be explained by quadratic functions of the concentrations of alanine, serine and glutamine supplied in the medium.

3.2. Reduction of feasible space using additional transport constraints

The metabolic capabilities of previously cryopreserved rat hepatocytes were investigated under a range of amino acid and hormone supplementation conditions. Following six days of preconditioning with high or low insulin provided, cultured hepatocytes were exposed to plasma-containing medium with varying amino acid and hormone supplementation levels for five days. At this time, the concentrations of extracellular metabolites in the supernatant and in the fresh medium were measured and used to calculate metabolic fluxes. The measured fluxes of metabolites in each culture condition are listed in Appendix D. The range of these experimental measurements defines the flux bounds $v_{\min} \leq v \leq v_{\max}$ covering all eight experiment settings (in Table 2).

Hepatocytes are multi-functional cells that must satisfy competing metabolic objectives; our prior work points to urea production and fatty acid oxidation as two examples [2]. In order to investigate the role of transport constraints on flux space, the bi-objective Pareto-optimal solutions (Model I) were first determined by finding the feasible boundary of urea production and fatty acid oxidation in cultured hepatocytes without transport constraints. The outline of the feasible range without transport constraints is represented by the lines A′B′C′D′ in Fig. 6, which shows the changes of flux values and directions from one objective to the other. By incorporating the transport constraints (Eqs. (2), (3) and (4)) to the bi-objective model (I), the feasible range of flux space is significantly reduced, which is represented by the line ABCD in Fig. 6.

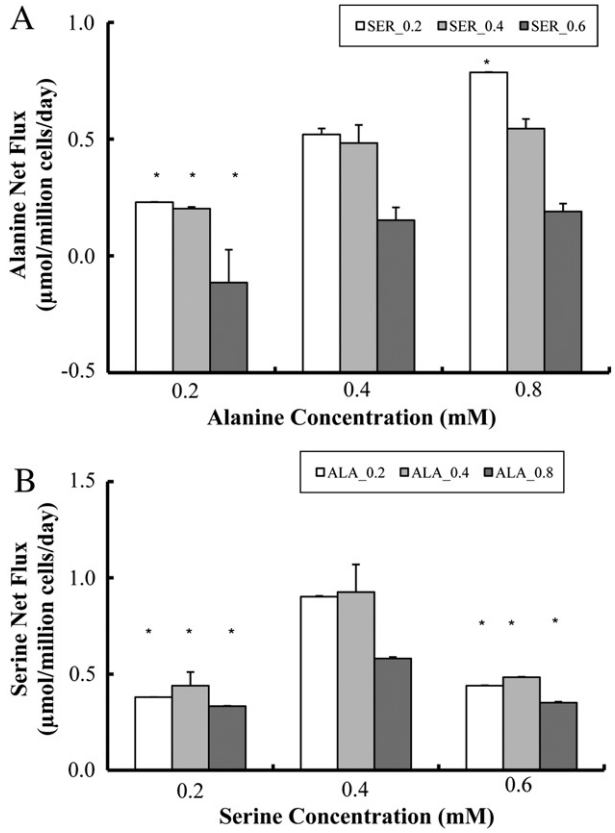

Fig. 3. Interplay of alanine and serine fluxes: (A) Alanine flux under varying combinations of alanine and serine concentrations in the medium. Asterisks (*) indicate significant differences ($p<0.05$) in fluxes between the indicated (A) alanine level and a supplied alanine level of 0.4 mM for the same glutamine and serine supplementation; or (B) serine level and a supplied serine level of 0.4 mM for the same glutamine and serine supplementation in the medium.

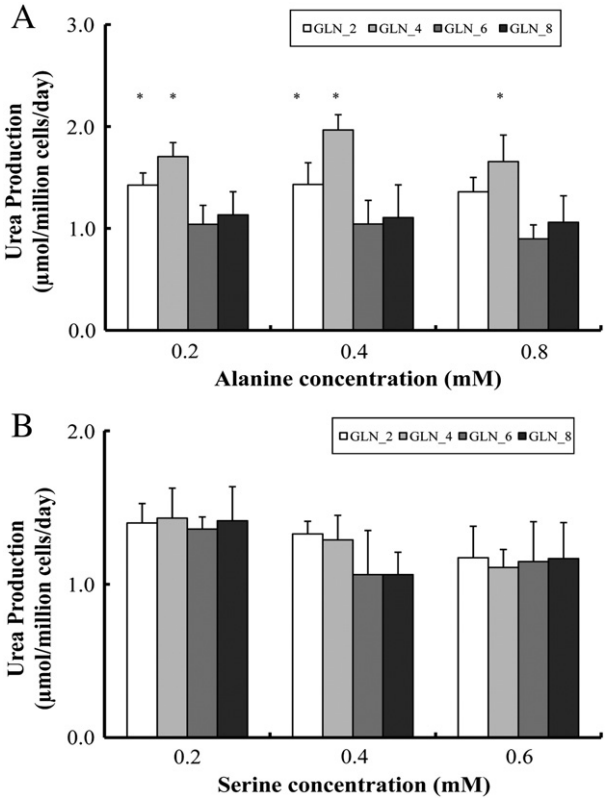

Fig. 4. Urea production (A) under varying combinations of alanine and glutamine supplementation; (B) under varying combinations of serine and glutamine supplementation. Asterisks (*) indicate significant differences ($p<0.05$) in urea production between the supplied glutamine level and a supplied glutamine level of 6 mM for the same alanine and serine supplementation.

3.3. Amino acid supplementation and flux distribution

The additional transport constraints significantly reduce the feasible region of the Pareto-optimal solution. By examining the whole feasible region in Fig. 6, from points A to B and from points C to D, an increase in one of the objectives (fatty acid oxidation flux or urea production) has a small effect on the other. However, a pronounced trade-off exists between points C and B, where an increase in urea production requires a large decrease in fatty acid oxidation. Point E in the feasible region corresponds to the results of the experiment in which hepatocytes were cultured with the designed amino acid supplementation. Both the urea and, to a lesser extent, fatty acid oxidation fluxes lie far from the boundary defined without transport constraints. The observed fluxes of urea and fatty acid oxidation lie closer to the flexibility envelope following incorporation of transport constraints, but they still do not lie at the boundary. This may indicate that the hepatocytes are not regulated in such a way as to maximize these functions, that other cellular functions not incorporated into the model necessitate compromise of these values, and/or that additional physicochemical constraints may exist.

Calculation of the flux distribution corresponding to different points in the Pareto-optimal solution provides insight into the connection between amino acid supplementation and the desired metabolic objectives. For example, point B corresponds to the maximum urea production with a secondary objective of high fatty acid oxidation flux and point F to the maximum urea production by maintaining the flux of fatty acid oxidation as that estimated from experimental data for designed amino acid supplementation and the flux balance framework (Yang et al., submitted for publication). Urea flux, fatty acid oxidation flux and the concentrations of alanine, serine and glutamine are calculated from the multi-objective model (II) and listed in Table 3, where they are compared with the experimental results with reference and designed amino acid supplementations (the complete flux distribution for point F is listed in Appendix E). According to the model calculation, glutamine supplementation should be reduced to 3.6 mM from 6.85 mM in reference and design amino acid supplementation, with relatively little change in alanine or serine concentrations (Table 3). This change in glutamine level is predicted to drive a doubling of urea production to 3.5 μmol/million cells/day while maintaining the same flux of fatty acid oxidation (2.8 μmol/million cells/day). This increase in urea production could be driven by an increase in pyruvate production, formed from alanine and serine. Pyruvate is further transformed to oxaloacetate and increases the flux of TCA cycle and urea cycle leading to a net increase in urea production.

4. Discussion

Amino acid supplementation can be used to induce an improvement in liver-specific functions of cultured hepatocytes during plasma exposure [1,2]. However, the levels of individual amino acids must be balanced for maximum effect. Furthermore, there are limits to the amount of supplementation possible due to the limited capacity and overlapping specificities of amino acid transporters. These considerations are important whether one is deriving a supplementation empirically or through the design approach based on flux balance optimization that we have proposed [2].

Compared with the concentrations of other amino acids (<1.5 mM), glutamine is supplied at a very high level to the plasma (6.85 mM) in both reference and designed amino acid supplementation. In cultured hepatocytes, glutamine is a key amino acid used to produce urea by

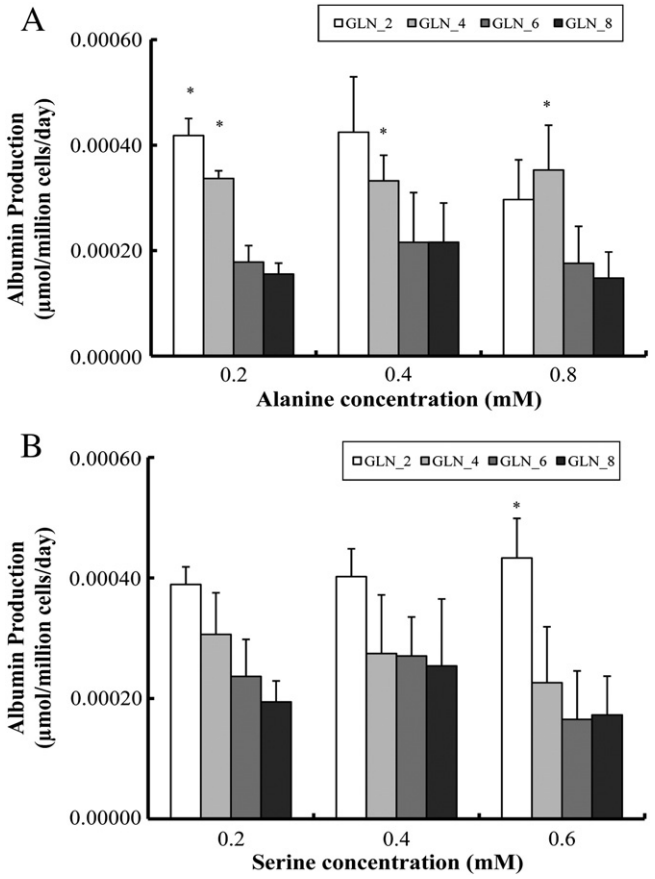

Fig. 5. Albumin production (A) under varying combinations of alanine and glutamine supplementation; (B) under varying combinations of serine and glutamine supplementation. Asterisks (*) indicate significant differences ($p<0.05$) in urea production between the supplied glutamine level and a supplied glutamine level of 6 mM for the same alanine and serine supplementation.

Table 2
Minimum and maximum values for measured fluxes with amino acid supplementation covering all eight experiment settings in Appendix D.

Metabolites		Flux bounds (μmol/million cells/day)	
		v_{min}	v_{max}
v_{m1}	Glucose	1.02	2.635
v_{m2}	Lactate	2.108	3.827
v_{m3}	Urea	0.562	10
v_{m4}	Arginine	0.105	0.647
v_{m5}	Ammonia	−1.311	0.025
v_{m6}	Ornithine	−0.556	−0.127
v_{m7}	Alanine	−10	10
v_{m8}	Serine	−10	10
v_{m9}	Cysterine	−0.00813	0.219
v_{m10}	Glycine	0.115	0.585
v_{m11}	Tyrosine	−0.76	0.207
v_{m12}	Glutamate	−1.783	−0.45
v_{m13}	Aspartate	−0.049	0.01
v_{m14}	Acetoacetate	0.116	0.235
v_{m15}	β-hydroxybutyrate	0.119	0.437
v_{m16}	Threonine	−0.887	0.664
v_{m17}	Lysine	−0.684	0.624
v_{m18}	Phenylalanine	−0.404	0.506
v_{m19}	Glutamine	0.23	100
v_{m20}	Proline	−1.843	0.574
v_{m21}	Methionine	−0.202	0.187
v_{m22}	Asparagine	−0.361	0.158
v_{m23}	Valine	−1.092	0.223
v_{m24}	Isoleucine	−0.937	−0.092
v_{m25}	Leucine	−0.8481	−0.003
v_{m26}	Albumin	0.000103	0.001452
v_{m27}	Glycerol	1.958	2.234
v_{m28}	Palmitate	0.796	1.093
v_{m29}	Cholesterol	0.543	2.216
v_{m30}	TG	0.694	0.946

deamidation of glutamine to glutamate via glutaminase, and glutamine requirements are also increased for patients with liver disease [22]. However, in this study, it is found that a maximum exists for glutamine supplementation, beyond which the liver-specific functions of urea and albumin production are compromised. It is also found that higher concentrations of glutamine inhibit the uptake of alanine and serine (Fig. 1), since these three amino acids share transport system A [6,9]. The reduction in uptake fluxes of alanine and serine is likely at least partially responsible for the reduction in the liver-specific functions of cultured hepatocytes (Figs. 3 and 4), since both of them serve as nitrogen sources for urea synthesis via pyruvate. Although hepatic glutamine transport is also mediated by system N, which allows uptake of histidine and asparagines in addition to glutamine, constraints arising from this system are not considered in this work since asparagine is supplied in a low level in both reference and designed amino acid supplementation (0.09 mM) and because both histidine and glutamine can be converted to glutamate.

In order to incorporate the observed transport limitations and interdependencies into the flux balance framework, three quadratic regression equations were developed. The quadratic representation captured the majority of the variance in the experimental data while retaining a form that can be solved fairly easily. To our knowledge, this is the first attempt to construct amino acid transport constraints in the field of flux balance analysis. The traditional constraints used in flux analysis include mass balances, reaction directionality and inequalities applied from the second law of thermodynamics on the individual reactions (energy balance analysis, EBA) [23] or on the pathways (standard pathway energy balance constraints [20,24], or minimum pathway energy balance constraints; Yang et al., submitted for publication). Employment of transport constraints provides an additional way to reduce the feasible range of the flux space and to predict more accurately the amount of amino acid supplementation in the medium by using nonlinear relationships among the relevant reaction fluxes and metabolites.

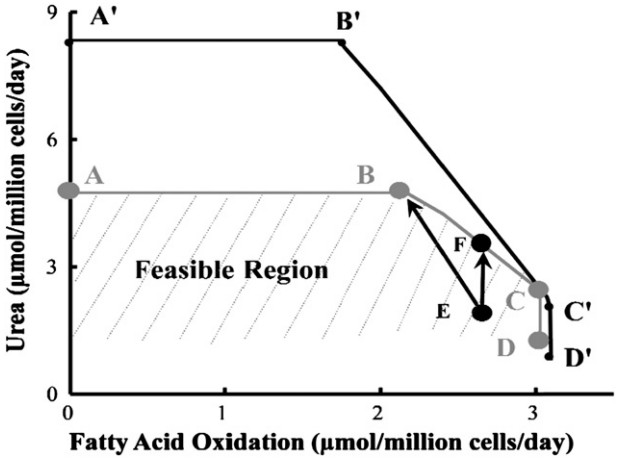

Fig. 6. Pareto-optimal solution for bi-objective problem in cultured hepatocytes: urea production vs. fatty acid oxidation. The solution without amino acid transport constraints is given in black, A′B′C′D′, and that with amino acid transport constraints is given in gray, ABCD. Point E is the experimentally observed point for designed amino acid supplementation. Point B and Point F are Pareto-solutions from bi-objective model (II) as discussed in the text.

Table 3
Amino acid supplementation in model and experiments.

	Model (II)		Experiments	
	Point 'B'	'Point F'	'DAA'	'RAA'
Urea production (μmol/million cells/day)	4.746	3.513	<1.7	<1.2
Fatty acid oxidation (μmol/million cells/day)	2.167	2.780	2.78	1.74
Alanine (mM)	0.57	0.50	0.46	0.29
Serine (mM)	0.33	0.41	0.36	0.10
Glutamine (mM)	2.67	3.38	6.85	6.85

We utilize flux balance analysis techniques both for design of amino acid supplementation as well as for interpretation of experimental results. Each activity informs the other. Experimental data are coupled with physicochemical constraints to design the amino acid supplementation. When such a supplementation is tested, new data are obtained that are not identical to the model predictions. Examination of the gaps between prediction and experiment leads to refinement of the model. This iterative process between model and experiment allows for the simultaneous increase in knowledge and improvement in performance of a cell culture. While there may be layers of cellular regulation that preclude facile incorporation into the model and thus a perfect match between theory and experiment, our results suggest that the approach is useful in addressing even complex metabolic systems such as cultured hepatocytes exposed to plasma.

Acknowledgments

We gratefully acknowledge the financial support from NSF QSB program (BES-0456697), NSF Metabolic Engineering (BES-0519563), and USEPA-funded Environmental Bioinformatics and Computational Toxicology Center (GAD R 832721-010). We also thank Aina Andrianarijaona for hepatocyte isolations, Vidya Iyer for help with the graphical abstract and François Berthiaume and Ioannis Androulakis for helpful discussions.

Appendix A

Transport/metabolic fluxes of alanine, serine and glutamine under various combinations of medium concentrations.

Concentration (mM)			Reaction Rate (μmol/10^6 cells/day) (measurement)		
[Ala]	[Ser]	[Gln]	Ala	Ser	Gln
0.2	0.2	1.5	0.2310	0.3795	1.0988
0.2	0.2	1.5	0.2289	0.3805	1.106
0.4	0.2	1.5	0.5384	0.4900	1.4665
0.4	0.2	1.5	0.5026	0.3893	1.0392
0.8	0.2	1.5	0.7856	0.3318	0.8739
0.8	0.2	1.5	0.7872	0.3344	0.8973
0.2	0.4	1.5	0.2078	0.9054	0.9811
0.2	0.4	1.5	0.1982	0.8996	–
0.4	0.4	1.5	0.5384	1.0277	1.4665
0.4	0.4	1.5	0.4292	0.8241	0.8739
0.8	0.4	1.5	0.516	0.5866	0.6068
0.8	0.4	1.5	0.5744	0.5753	0.6013
0.2	0.6	1.5	−0.2135	0.4385	0.4789
0.2	0.6	1.5	−0.0146	0.4407	0.4431
0.4	0.6	1.5	0.114	0.4813	0.5762
0.4	0.6	1.5	0.1916	0.4855	0.516
0.8	0.6	1.5	0.2144	0.3485	0.1378
0.8	0.6	1.5	0.1666	0.3548	0.2532
0.2	0.1	2	0.2135	0.0605	1.4193
0.2	0.1	2	0.2316	–	1.4005
0.4	0.1	2	0.4568	0.0396	1.3162
0.4	0.1	2	0.4553	0.0464	1.3662
0.8	0.1	2	0.6619	0.0004	1.1345
0.8	0.1	2	0.6805	0.0062	1.2532

Appendix A (*continued*)

Concentration (mM)			Reaction Rate (μmol/10^6 cells/day) (measurement)		
[Ala]	[Ser]	[Gln]	Ala	Ser	Gln
0.2	0.1	4	0.2386	−0.0119	2.9747
0.2	0.1	4	0.2398	−0.0673	3.0813
0.4	0.1	4	0.4987	−0.0832	2.4495
0.4	0.1	4	0.486	−0.0003	2.4439
0.8	0.1	4	0.6893	−0.0036	2.9721
0.8	0.1	4	0.7003	−0.0003	3.0334
0.2	0.1	6	−0.5883	−0.1699	2.7946
0.2	0.1	6	−0.5734	−0.1519	2.8807
0.4	0.1	6	−0.0672	–	3.2177
0.4	0.1	6	−0.0666	–	3.2476
0.8	0.1	6	−0.2354	−0.1934	2.7653
0.8	0.1	6	−0.2251	−0.178	2.6747
0.2	0.1	8	−0.9394	−0.1504	2.9943
0.2	0.1	8	−0.8807	−0.1559	3.1568
0.4	0.1	8	−0.6733	−0.1573	3.2043
0.4	0.1	8	−0.6595	−0.1448	3.3048
0.8	0.1	8	−0.4046	−0.1531	3.2694
0.8	0.1	8	−0.3809	−0.1435	3.4830
0.1	0.2	2	0.0424	0.1128	1.4834
0.1	0.2	2	0.0181	0.0503	1.286
0.1	0.4	2	0.0019	0.2443	1.427
0.1	0.4	2	−0.0441	0.1554	1.1554
0.1	0.6	2	0.0407	0.2738	1.4501
0.1	0.6	2	0.0011	0.1828	1.2113
0.1	0.2	4	−0.1923	−0.0371	2.6702
0.1	0.4	4	−0.3981	0.0331	2.5339
0.1	0.4	4	−0.3079	−0.0169	2.5510
0.1	0.6	4	−0.4093	−0.0096	2.5737
0.1	0.6	4	−0.3037	0.0324	2.6463
0.1	0.2	6	−0.7439	−0.1664	2.9524
0.1	0.2	6	–	−0.1537	2.7910
0.1	0.4	6	−0.7361	−0.0739	2.7299
0.1	0.4	6	−0.6732	−0.0543	2.7700
0.1	0.6	6	−0.392	−0.0748	3.0141
0.1	0.6	6	−0.7048	−0.0490	3.0051
0.1	0.2	8	−1.0355	−0.1783	3.0370
0.1	0.2	8	−0.96	−0.1586	2.7833
0.1	0.4	8	−0.7878	−0.0322	3.1341
0.1	0.4	8	−0.8291	−0.0034	3.0526
0.1	0.6	8	−0.9315	−0.1354	3.2511
0.1	0.6	8	−0.8231	−0.0978	3.2025

Missing values, denoted by –, are those for which the designated amino acid peak could not be distinguished from a neighboring peak on HPLC.

Appendix B

Concentrations of amino acids in culture media[a] (mM).

	RAA	DAA
L-arginine	0.42	0.56
L-alanine	0.29	0.46
L-serine	0.10	0.36
L-threonine	0.79	1.18
L-valine	0.87	1.49
L-isoleucine	0.78	0.89
L-leucine	0.83	1.02
L-histidine	0.35	0.44
L-glycine	0.17	0.41
L-lysine	0.75	0.79
L-proline	0.18	0.22
L-tyrosine	0.40	0.72
L-glutamate	0.11	0.11
L-aspartate	0.01	0.01
L-cysteine	0.13	0.13
L-phenylalanine	0.42	0.42
L-glutamine	6.85	6.85
L-methionine	0.20	0.20
L-asparagine	0.09	0.09

[a] Values shown represent final concentrations of amino acid supplementation during plasma exposure in the experimental design. RAA = "reference" amino acid supplementation; DAA = "designed" amino acid supplementation.

Appendix C

Hepatic metabolic network.

No. and enzyme	Stoichiometry
Measurement fluxes	
v_{m1} Hexokinase	$Glucose + P_i \rightarrow Glucose\text{-}6\text{-}P + H_2O$
v_{m2} Lactate dehydrogenase	$Lactate + NAD^+ \leftrightarrow Pyruvate + NADH + H^+$
v_{m3} Arginase	$Arginine + H_2O \rightarrow Urea + Ornithine$
v_{m4}	Arginine uptake
v_{m5}	NH_4^+ uptake
v_{m6}	Ornithine secretion
v_{m7}	Alanine uptake
v_{m8}	Serine uptake
v_{m9}	Cysteine uptake
v_{m10}	Glycine uptake
v_{m11}	Tyrosine uptake
v_{m12}	Glutamate uptake
v_{m13}	Aspartate uptake
v_{m14}	Acetoacetate production
v_{m15}	$Acetoacetate + NADH + H^+ \leftrightarrow \beta\text{-OH-butyrate} + NAD^+$
v_{m16}	Threonine uptake
v_{m17}	Lysine uptake
v_{m18}	Phenylalanine uptake
v_{m19}	Glutamine uptake
v_{m20}	Proline uptake
v_{m21}	Methionine uptake
v_{m22}	Asparagine uptake
v_{m23}	Valine uptake
v_{m24}	Isoleucine uptake
v_{m25}	Leucine uptake
v_{m26}	Albumin synthesis
v_{m27}	Glycerol uptake
v_{m28}	Palmitate uptake
v_{m29} Cholesterol esterase	$Cholesterol\ ester + H_2O \rightarrow Cholesterol + Palmitate$
v_{m30}	TG uptake
Unknown fluxes	
v_{u1} Phosphoglucose isomerase	$Glucose\text{-}6\text{-}P \leftrightarrow Fructose\text{-}6\text{-}P$
v_{u2} PFK-1	$Fructose\text{-}6\text{-}P + P_i \rightarrow Fructose\text{-}1,6\text{-}P_2 + H_2O$
v_{u3} Two Steps	$Fructose\text{-}1,6\text{-}P_2 \leftrightarrow 2\ Glyceraldehyde\text{-}3\text{-}P$
v_{u4} Four Steps	$Glyceraldehyde\text{-}3\text{-}P + P_i + NAD^+ + ADP \leftrightarrow Phosphoenolpyruvate + NADH + H^+ + ATP + H_2O$
v_{u5} Pyruvate kinase	$Phosphoenolpyruvate + ADP \rightarrow pyruvate + ATP$
v_{u6} PDH	$Pyruvate + CoA + NAD^+ \rightarrow Acetyl\text{-}CoA + CO_2 + NADH$
v_{u7} Citrate synthase	$Oxaloacetate + Acetyl\text{-}CoA + H_2O \rightarrow Citrate + CoA + H^+$
v_{u8} Isocitrate dehydrogenase	$Citrate + NAD^+ \leftrightarrow \alpha\text{-ketoglutarate} + CO_2 + NADH$
v_{u9} α-ketoglutarate dehydrogenase	$NAD^+ + \alpha\text{-ketoglutarate} + CoA \rightarrow Succinyl\text{-}CoA + CO_2 + NADH + H^+$
v_{u10} Succinyl-CoA synthetase, succinate dehydrogenase	$Succinyl\text{-}CoA + P_i + GDP + FAD \leftrightarrow Fumarate + GTP + FADH_2 + CoA$
v_{u11} Fumarase	$Fumarate + H_2O \leftrightarrow Malate$
v_{u12} Malate dehydrogenase	$Malate + NAD^+ \leftrightarrow Oxaloacetate + NADH + H^+$
v_{u13} Carbamoyl-P-synthetase I, ornithine transcabamylase	$Ornithine + CO_2 + NH_4^+ + 2ATP + H_2O \leftrightarrow Citrulline + 2ADP + 2P_i + 3H^+$
v_{u14}Argininosuccinase, Argininosuccinate synthetase	$Citrulline + Aspartate + ATP \rightarrow Arginine + Fumarate + AMP + PP_i$
v_{u15} Alanine aminotransferase	$Alanine + 0.5\ NAD^+ + 0.5\ NADP^+ + H_2O \rightarrow Pyruvate + NH_4^+ + 0.5\ NADPH + 0.5\ NADH + H^+$
v_{u16}	$Serine \rightarrow NH_4^+ + Pyruvate$
v_{u17} 3-mercaptopyruvate sulfurtransferase, transminase	$Cysteine + 0.5\ NAD^+ + 0.5\ NADP^+ + H_2O + SO_3^{2-} \leftrightarrow Pyruvate + Thiosulfate + NH_4^+ + 0.5\ NADH + 0.5\ NADPH + H^+$
v_{u18} Serine hydroxymethyl transferase	$Threonine + NAD^+ \rightarrow Glycine + Acetyl\text{-}CoA + NADH$
v_{u19} Glycine DH, Aminomethytransferase, dihydrolipoyl DH Aminomethytransferase,	$Glycine + NAD^+ + H_4folate \leftrightarrow Serine + N^5,N^{10}\text{–}CH_2\text{–}H_4folate + NADH + NH_4^+$
v_{u20} Nine Steps	$Tryptophan + 3H_2O + 3O_2 + CoA + 3NAD^+ + FAD \rightarrow 3CO_2 + FADH_2 + 3NADH + 4H^+ + NH_4^+ + Acetoacetyl\text{-}CoA$
v_{u21} Three Steps	$Propionyl\text{-}CoA + ATP + CO_2 \rightarrow Succinyl\text{-}CoA + AMP + PP_i$
v_{u22} Eight Steps	$Lysine + 3H_2O + 5NAD^+ + FAD + CoA \rightarrow 2NH_4^+ + 5H^+ + 5NADH + 2CO_2 + FADH_2 + Acetoacetyl\text{-}CoA$
v_{u23} Phenylalanine hydroxylase	$Phenylalanine + H_4biopterin + O_2 \rightarrow H_2biopterin + Tyrosine + H_2O$
v_{u24} Five steps	$Tyrosine + 0.5NAD^+ + 0.5NADP^+ + H_2O + 2O_2 \rightarrow NH_4^+ + 0.5NADH + 0.5NADPH + H^+ + CO_2 + Fumarate + Acetoacetate$
v_{u25} Glutamate dehydrogenase I	$Glutamate + 0.5NAD^+ + 0.5NADP^+ + H_2O \leftrightarrow NH_4^+ + \alpha\text{-ketoglutarate} + 0.5NADP + 0.5NADPH + H^+$
v_{u26} Glutaminase	$Glutamine + H_2O \rightarrow Glutamate + NH_4^+$
v_{u27}Two steps	$Ornithine + NAD^+ + NADP^+ + H_2O \rightarrow Glutamate + NH_4^+ + NADH + NADPH + H^+$
v_{u28} Three steps	$Proline + 0.5\ O_2 + 0.5NAD^+ + 0.5NADP^+ \rightarrow Glutamate + 0.5NADH + 0.5NADPH + H^+$
v_{u29} Four steps	$Histidine + H_4folate + 2H_2O \rightarrow NH_4^+ + N^5\text{-}formiminoH_4folate + Glutamate$
v_{u30} Five steps	$Methionine + ATP + Serine + NAD^+ + CoA \rightarrow PP_i + P_i + Adenosine + Cysteine + NADH + CO_2 + NH_4^+ + Propionyl\text{-}CoA$

Appendix C (*continued*)

No. and enzyme	Stoichiometry
Unknown fluxes	
v_{u31} Aspartate aminotransferase	$Aspartate + 0.5NAD^+ + 0.5NADP^+ + H_2O \leftrightarrow Oxaloacetate + NH_4^+ + 0.5NADH + 0.5NADPH + H^+$
v_{u32} Asparaginase	$Asparagine + H_2O \rightarrow Aspartate + NH_4^+$
v_{u33} Fatty acid oxidation	$Palmitate + ATP + 7FAD + 7NAD^+ + 8CoA \rightarrow 8acetyl\text{-}CoA + 7FADH_2 + 7NADH + AMP + PP_i$
v_{u34} Thiolase	$2Acetyl\text{-}CoA \leftrightarrow Acetoacetyl\text{-}CoA + CoA$
v_{u35}Two steps	$Acetoacetyl\text{-}CoA + H_2O \rightarrow Acetoacetate + CoA$
v_{u36} ECT	$NADH + H^+ + 0.5O_2 + 3ADP \rightarrow NAD^+ + H_2O + 3ATP$
v_{u37} ECT	$FADH_2 + 0.5O_2 + 2ADP \rightarrow FAD + H_2O + 2ATP$
v_{u38} Glucose-6-P-dehydrogenase	$Glucose\text{-}6\text{-}P + 12NADP^+ + 7H_2O \rightarrow 6CO_2 + 12NADPH + 12H^+ + P_i$
v_{u39} Seven steps	$Valine + 0.5NADP^+ + CoA + 2H_2O + 3.5NAD^+ + FAD \rightarrow NH_4^+ + 0.5NADPH + 3H^+ + 3.5NADH + FADH_2 + 2CO_2 + Propionyl\text{-}CoA$
v_{u40} Six steps	$Isoleucine + 0.5NADP^+ + 2H_2O + 2.5NAD^+ + FAD + 2CoA \rightarrow NH_4^+ + 0.5NADPH + 3H^+ + 2.5NADH + FADH_2 + CO_2 + Propionyl\text{-}CoA + Acetyl\text{-}CoA$
v_{u41} Six steps	$Leucine + 0.5NADP^+ + H_2O + 1.5NAD^+ + FAD + ATP + CoA \rightarrow NH_4^+ + 1.5NADH + 0.5NADPH + 2H^+ + FADH_2 + ADP + P_i + Acetoacetate + Acetyl\text{-}CoA$
v_{u42} Lipoprotein and hepatic lipase	$TG + 3H_2O \rightarrow Glycerol + 3Palmitate + 3H^+$
v_{u43} Three steps	$Glucose\text{-}6\text{-}P + UTP + H_2O \rightarrow Glycogen + 2P_i + UDP$
v_{u44}Glycerol-3-P-dehydrogenase	$Glycerol + NAD^+ \leftrightarrow Glyceraldehyde\text{-}3\text{-}P + NADH + H^+$
v_{u45}	TG store
v_{u46}	O_2 uptake
v_{u47}	Histidine uptake
v_{u48}	Tryptophan uptake

Appendix D

Measurement data from experiment of amino acid supplementation.

	Flux rate (μmol/million cells/day)*							
	Without hormones (NH)				With hormone supplementation (WH)			
	RAA		DAA		RAA		DAA	
	HI	LI	HI	LI	HI	LI	HI	LI
1	0.563 ± 0.439	1.284 ± 0.183	1.614 ± 0.609	2.51 ± 0.125	1.003 ± 0.502	0.548 ± 0.121	1.195 ± 0.343	0.668 ± 0.352
2	3.074 ± 0.04	3.013 ± 0.115	2.197 ± 0.089	3.525 ± 0.07	3.107 ± 0.128	3.202 ± 0.36	2.327 ± 0.064	3.467 ± 0.36
3	0.838 ± 0.131	0.718 ± 0.156	1.556 ± 0.049	1.192 ± 0.131	1.117 ± 0.13	1.18 ± 0.051	1.459 ± 0.246	1.504 ± 0.182
4	0.338 ± 0.008	0.396 ± 0.007	0.269 ± 0.023	0.125 ± 0.02	0.611 ± 0.012	0.545 ± 0.012	0.635 ± 0.012	0.565 ± 0.014
5	0.022 ± 0.003	−0.061 ± 0.009	−0.52 ± 0.021	−1.128 ± 0.025	−0.467 ± 0.003	−0.78 ± 0.001	−1.294 ± 0.017	−1.011 ± 0.019
6	−0.548 ± 0.008	−0.286 ± 0.004	−0.442 ± 0.009	−0.376 ± 0.004	−0.132 ± 0.005	−0.336 ± 0.004	−0.349 ± 0.005	−0.521 ± 0.034
7	0.224 ± 0.024	0.243 ± 0.024	−0.041 ± 0.017	−0.203 ± 0.017	0.139 ± 0.006	−0.169 ± 0.009	0.043 ± 0.012	−0.313 ± 0.013
8	−0.389 ± 0.008	−0.238 ± 0.006	−0.779 ± 0.029	−0.738 ± 0.021	−0.075 ± 0.003	−0.347 ± 0.006	−0.341 ± 0.014	−0.679 ± 0.023
9	0.127 ± 0.019	0.211 ± 0.008	0.057 ± 0.005	0.073 ± 0.006	0.111 ± 0.0038	0.0661 ± 0.012	0.0396 ± 0.014	0.0019 ± 0.010
10	0.195 ± 0.006	0.218 ± 0.003	0.32 ± 0.027	0.128 ± 0.013	0.258 ± 0.004	0.246 ± 0.004	0.576 ± 0.009	0.53 ± 0.009
11	−0.185 ± 0.014	0.004 ± 0.011	−0.667 ± 0.046	−0.729 ± 0.031	0.17 ± 0.03	0.028 ± 0.014	0.184 ± 0.023	−0.233 ± 0.059
12	−1.083 ± 0.024	−0.602 ± 0.014	−1.211 ± 0.032	−1.104 ± 0.019	−0.456 ± 0.006	−1.459 ± 0.02	−1.448 ± 0.02	−1.752 ± 0.031
13	−0.014 ± 0.001	−0.005 ± 0.001	−0.027 ± 0.002	−0.047 ± 0.002	0.009 ± 0.001	−0.021 ± 0.001	−0.017 ± 0.001	−0.03 ± 0.001
14	0.2 ± 0.035	0.19 ± 0.042	0.2 ± 0.034	0.15 ± 0.001	0.18 ± 0.006	0.14 ± 0.024	0.16 ± 0.018	0.15 ± 0.009
15	0.328 ± 0.015	0.4 ± 0.037	0.214 ± 0.052	0.267 ± 0.025	0.148 ± 0.015	0.158 ± 0.018	0.15 ± 0.031	0.16±.0009
16	−0.699 ± 0.031	−0.077 ± 0.017	−0.833 ± 0.054	−0.764 ± 0.045	0.643 ± 0.021	0.207 ± 0.023	−0.041 ± 0.03	−0.451 ± 0.044
17	−0.66 ± 0.024	−0.126 ± 0.015	−0.344 ± 0.03	−0.414 ± 0.024	0.604 ± 0.02	−0.067 ± 0.023	−0.094 ± 0.014	−0.451 ± 0.026
18	−0.337 ± 0.015	−0.001 ± 0.009	−0.38 ± 0.024	−0.345 ± 0.017	0.493 ± 0.013	0.326 ± 0.013	0.289 ± 0.012	0.107 ± 0.013
19	2.622 ± 1.283	2.622 ± 1.283	2.846 ± 1.083	2.846 ± 1.083	2.666 ± 0.688	2.768 ± 0.538	2.173 ± 0.777	1.799 ± 0.717
20	−0.816 ± 0.528	−0.763 ± 0.028	−1.094 ± 0.367	−1.289 ± 0.554	0.417 ± 0.033	0.475 ± 0.037	0.419 ± 0.119	0.463 ± 0.111
21	−0.181 ± 0.006	−0.017 ± 0.004	−0.168 ± 0.01	−0.191 ± 0.011	0.122 ± 0.008	0.011 ± 0.01	0.152 ± 0.035	−0.045 ± 0.06
22	−0.088 ± 0.005	0.103 ± 0.055	−0.331 ± 0.03	−0.313 ± 0.01	−0.02 ± 0.005	0.081 ± 0.005	−0.046 ± 0.007	−0.134 ± 0.006
23	−1.072 ± 0.02	−0.356 ± 0.011	−0.778 ± 0.044	−0.786 ± 0.041	–	−0.197 ± 0.022	−0.034 ± 0.257	−0.654 ± 0.026
24	−0.92 ± 0.017	−0.261 ± 0.011	−0.728 ± 0.044	−0.74 ± 0.041	–	−0.32 ± 0.022	−0.119 ± 0.257	−0.469 ± 0.026
25	−0.827 ± 0.021	−0.247 ± 0.009	−0.712 ± 0.03	−0.743 ± 0.025	–	−0.013 ± 0.02	−0.092 ± 0.023	−0.441 ± 0.037
26	0.517 ± 0.002	0.192 ± 0.089	0.548 ± 0.057	0.185 ± 0.078	0.049 ± 0.085	0.708 ± 0.165	1.245 ± 0.207	1.091 ± 0.042
27	2.001 ± 0.007	2.044 ± 0.014	1.983 ± 0.025	2.075 ± 0.042	2.021 ± 0.023	2.107 ± 0.127	2.048 ± 0.018	2.075 ± 0.007
28	1.012 ± 0.019	1.071 ± 0.022	0.992 ± 0.009	0.812 ± 0.016	0.983 ± 0.092	1.073 ± 0.008	1.07 ± 0.003	0.981 ± 0.005
29	1.944 ± 0.27	1.422 ± 0.10	1.759 ± 0.056	1.864 ± 0.352	0.778 ± 0.099	0.671 ± 0.128	0.801 ± 0.225	0.753 ± 0.208
30	0.84 ± 0.003	0.85 ± 0.022	0.87 ± 0.02	0.88 ± 0.01	0.84 ± 0.057	0.82 ± 0.126	0.830 ± 034	0.92 ± 0.014

* Except albumin flux (v_{26}), which is in units of nmol/million cells/day.

Appendix E

Intracellular flux distribution from model (II).

#	Flux rate (μmol/million cells/day)
Gluconeogenesis pathway, PPP, glycogen storage	
v_{u1}, v_{u2}, v_{u3}	0.48
v_{u4}, v_{u5}	3.05
v_{u6}	7.20
v_{u38}	0.14
v_{u43}	0.40
TCA cycle	
v_{u7}, v_{u8}	26.33
v_{u9}	26.33
v_{u10}	27.09
v_{u11}, v_{u12}	29.20
Urea cycle	
v_{u13}, v_{u14}	2.90
Amino acid catabolism	
v_{u15}	0.12
v_{u16}	1.50
v_{u17}	0.16
v_{u18}	0.62
v_{u19}	1.18
v_{u20}	0.73
v_{u24}	−0.40
v_{u25}	0.38
v_{u26}	2.15
v_{u27}	0.06
v_{u29}	0.42
v_{u30}	0.18
v_{u31}	−1.43
v_{u32}	0.13
Amino acid catabolism	
v_{u40}	−0.09
v_{u41}	−0.47
v_{u47}	0.44
v_{u48}	0.73
Fatty acid, lipid and glycerol metabolism	
v_{u33}	2.78
v_{u34}	1.31
v_{u35}	2.04
v_{u42}	0.13
v_{u44}	2.09
v_{u45}	0.56
Oxygen uptake, electron transport system	
v_{u36}	58.65
v_{u37}	23.09

References

[1] C. Chan, D. Hwang, G.N. Stephanopoulos, M.L. Yarmush, G. Stephanopoulos, Application of multivariate analysis to optimize function of cultured hepatocytes, Biotechnol Prog 19 (2003) 580–598.

[2] H. Yang, C.M. Roth, M.G. Ierapetritou, A rational design approach for amino acid supplementation in hepatocyte culture, Biotechnol Bioeng 103 (2009) 1176–1191.

[3] M.S. Malandro, M.S. Kilberg, Molecular biology of mammalian amino acid transporters, Annu Rev Biochem 65 (1996) 305–336.

[4] M. Palacin, R. Estevez, J. Bertran, A. Zorzano, Molecular biology of mammalian plasma membrane amino acid transporters, Physiol Rev 78 (1998) 969–1054.

[5] R. Hyde, P.M. Taylor, H.S. Hundal, Amino acid transporters: roles in amino acid sensing and signalling in animal cells, Biochem J 373 (2003) 1–18.

[6] S.K. Joseph, N.M. Bradford, J.D. McGivan, Characteristics of the transport of alanine, serine and glutamine across the plasma membrane of isolated rat liver cells, Biochem J 176 (1978) 827–836.

[7] P. Fafournoux, C. Remesy, C. Demigne, Control of alanine metabolism in rat liver by transport processes or cellular metabolism, Biochem J 210 (1983) 645–652.

[8] D. Haussinger, S. Soboll, A.J. Meijer, W. Gerok, J.M. Tager, H. Sies, Role of plasma membrane transport in hepatic glutamine metabolism, Eur J Biochem 152 (1985) 597–603.

[9] H.N. Christensen, D.L. Oxender, M. Liang, K.A. Vatz, The use of N-methylation to direct route of mediated transport of amino acids, J Biol Chem 240 (1965) 3609–3616.

[10] J.C. Dunn, R.G. Tompkins, M.L. Yarmush, Long-term in vitro function of adult hepatocytes in a collagen sandwich configuration, Biotechnol Prog 7 (1991) 237–245.

[11] G.N. Stephanopoulos, A.A. Aristidou, J. Nielsen, Metabolic Engineering: Principles and Methodologies, Academic Press, San Diego, CA, 1998.

[12] K. Lee, F. Berthiaume, G.N. Stephanopoulos, M.L. Yarmush, Profiling of dynamic changes in hypermetabolic livers, Biotechnol Bioeng 83 (2003) 400–415.

[13] D. Nagrath, M. Avila-Elchiver, F. Berthiaume, A.W. Tilles, A. Messac, M.L. Yarmush, Integrated energy and flux balance based multiobjective framework for large-scale metabolic networks, Ann Biomed Eng 35 (2007) 863–885.

[14] K. Uygun, H.W. Matthew, Y. Huang, Investigation of metabolic objectives in cultured hepatocytes, Biotechnol Bioeng 97 (2007) 622–637.

[15] N.S. Sharma, M.G. Ierapetritou, M.L. Yarmush, Novel quantitative tools for engineering analysis of hepatocyte cultures in bioartificial liver systems, Biotechnol Bioeng 92 (2005) 321–335.

[16] A. Marin-Sanguino, N.V. Torres, Optimization of tryptophan production in bacteria. Design of a strategy for genetic manipulation of the tryptophan operon for tryptophan flux maximization, Biotechnol Prog 16 (2000) 133–145.

[17] V.V. Iyer, M.A. Ovacik, I.P. Androulakis, C.M. Roth, M.G. Ierapetritou, Transcriptional and metabolic flux profiling of triadimefon effects on cultured hepatocytes, Toxicol Appl Pharmacol (2010), doi:10.1016/j.taap.2010.07.015.

[18] M. Kanehisa, S. Goto, KEGG: Kyoto encyclopedia of genes and genomes, Nucleic Acids Res 28 (2000) 27–30.

[19] Y.Y. Haimes, U. Lasdon, D.A. Wismer, On a bicriterion formulation of the problems of integrated system identification and system optimization, IEEE Trans Syst Man Cybern 1 (1971) 296–297.

[20] V.V. Iyer, H. Yang, M.G. Ierapetritou, C.M. Roth, Effects of glucose and insulin on HepG2-C3A cell metabolism, Biotechnol Bioeng 107 (2010) 347–356.

[21] J. Washizu, F. Berthiaume, C. Chan, R.G. Tompkins, M. Toner, M.L. Yarmush, Optimization of rat hepatocyte culture in citrated human plasma, J Surg Res 93 (2000) 237–246.

[22] D. Darmaun, Role of glutamine depletion in severe illness, Diabetes Nutr Metab 13 (2000) 25–30.

[23] D.A. Beard, H. Qian, Thermodynamic-based computational profiling of cellular regulatory control in hepatocyte metabolism, Am J Physiol Endocrinol Metab 288 (2005) E633–E644.

[24] R.P. Nolan, A.P. Fenley, K. Lee, Identification of distributed metabolic objectives in the hypermetabolic liver by flux and energy balance analysis, Metab Eng 8 (2006) 30–45.

[25] S. Gu, H.L. Roderick, P. Camacho, J.X. Jiang, Identification and characterization of an amino acid transporter expressed differentially in liver, Proc Natl Acad Sci USA 97 (2000) 3230–3235.

[26] S. Gu, C.J. Villegas, J.X. Jiang, Differential regulation of amino acid transporter SNAT3 by insulin in hepatocytes, J Biol Chem 280 (2005) 26055–26062.